https://doi.org/10.30799/jnst.337.22080401 J. Nanosci. Tech. - Volume 8 Issue 4 (2022) 967–971

Share Your Innovations through JACS Directory

Journal of Nanoscience and Technology

Visit Journal at https://www.jacsdirectory.com/jnst

ISSN: 2455-0191

Electrochemical Synthesis and Characterization of CdO/CuO Nanocomposite: Photocatalytic Degradation Kinetics of Indigo Carmine Dye and Its Antimicrobial-Anticancer Activities

H.S. Sindhushree, K.M. Chaithra, B.M. Venkatesha*

Department of Chemistry, Yuvaraja's College, University of Mysore, Mysuru – 570 005, Karnataka, India.

ARTICLEDETAILS

Article history:
Received 21 November 2022
Accepted 15 December 2022
Available online 28 December 2022

Keywords:
Electrochemical Method
CdO/CuO Nanocomposite
Indigo Carmine Dye
Antibacterial Activity

ABSTRACT

In the few decades use of nanostructured material have received a considerable importance because of its effective biological application. Therefore nanostructured CdO/CuO nanocomposite photocatalyst synthesized by electrochemical method, which is simple and inexpensive method. The characterization techniques included are UV-visible spectroscopy, SEM-EDAX, and X-ray diffraction techniques. From UV-visible spectroscopy and by using Tauc plot the band gap energy of CdO/CuO nanocomposite is calculated and found to be 4.56 eV. The SEM results show that the synthesized nanocomposite have agglomerated particles. The EDAX spectra showed that the presence of cadmium, oxygen and copper in the synthesized nanocomposite. From the XRD data and with the help of Debye-Scherrer's formula the crystalline size is calculated and found to be ≈ 49.56 nm. The photocatalytic activity of the synthesized nanocomposite was examined by the kinetics of photodegradation of indigo carmine dye. The degradation efficiency investigated was found as ≈97%. The antimicrobial and anticancer activities were evaluated for the synthesized CdO/CuO nanocomposite against the control.

1. Introduction

Over the past few decades, the use of nanostructured material is becoming more wide spread due to its miraculous and curious application in the branch of chemistry, pharmacy, agriculture, textile, optoelectronics, physics and so on [1]. The research of nanostructures can deliver extraordinary understanding of materials and devices, nanostructures reveal novel and significantly improved physicochemical properties, and processes compared to their majority counterparts. Nanomaterial has widely differing qualities beyond what they exhibit at the macro or micro sizes due to its unique features, and they will be widely employed in several applications [2]. There are many methods for the synthesis of nanoparticles such as: vapour deposition, electrochemical method, combustion, colloid thermal synthesis process, microwave irradiation, thermal oxidation, pulsed wire explosion methods, precipitation, and sol-gel. The electrochemical method is considered as one of the most important and famous technique to synthesis nanoparticle [3-7]. It is important to develop novel synthesis methods to fabricate nanostructured materials useful for new technological applications. Investigations of properties of new nanostructures synthesized by the addition of cadmium oxide metal were carried out [8]. The high intrinsic durability of CdO nanoparticles coupled with magnificent mobility gives high electrical conductivity due to the presence of shallow benefactors conveyed by intrinsic interstitial cadmium atoms and oxygen vacancies. CdO nanoparticle is an n-type semiconductor with a direct band gap of 2.3 eV, and an indirect one of 1.36 eV. The nanostructure materials of CdO nanoparticles can play an important role in order to get cost effective and high-performance supercapacitor electrode materials due to their extensive surface area-to-volume ratio and conducting nature [9-11]. Cadmium oxide (CdO) nanoparticles are also used for drug delivery to cancer cells. However, due to the very tiny size of the cadmium oxide (CdO) nanoparticles, each can carry only small amounts of the drug. Therefore, it is necessary to utilize millions or even billions of these nanoparticles for drug delivery to the exact cancer location. In this way, difficulty to deliver anti–cancer drug to the desired location will be resolved without affecting healthy cells. Recently, successful application of cadmium Oxide (CdO) nanoparticles in the early detection of cancer cells has been shown. Furthermore, a sensor has been made by cadmium Oxide (CdO) nanoparticles which can identify lung cancer through patient breath. At the moment, the accuracy of the device which has been tested on a group of healthy individuals and individuals with cancer is 86 percent [12-14].

2. Experimental Methods

2.1 Chemicals and Characterization

All the chemicals, used to prepare CdO/CuO nanocomposite, were the analytical grades of purity. Cd and Cu wire were purchased from Alfa Aesar. Indigo carmine dye from lobachemie, platinum electrode from Elico Pvt. Ltd. All solutions were prepared with double distilled water. The optical properties for prepared CdO/CuO nanocomposite were studied by UV-visible spectrophotometer (shimadzu-1700 series). The X-ray crystallographic interpretations were performed by X-ray diffractometer (Panalytical X-Pert) using Cu Ka wavelength (λ=1.54) scanning range from 0 to 700. The morphological feature for the prepared CdO/CuO nanocomposite study had determined by scanning electron microscopy (SEM-EDEX) from quanta-200 FEI, Netherlands. The elemental analysis for the confirmation of prepared Cd, Cu and O is confirmed from energy dispersive X-ray analysis (EDAX).

2.2 Synthesis of CdO/CuO Nanocomposite by Electrochemical Method

The CdO/CuO nanocomposite is synthesized by electrochemical method. The experimental process is as shown in Fig. 1. The transition Cd and Cu metal wire is used as anode and platinum electrode is used as cathode. Using 15 mA current and potential of 10 V the experiment was run for 2 hrs with continuous stirring. The electrolytic cell is consisting of 5 % of aqueous $NaHCO_3$ solution. The distance of the anode and cathode during electrolysis was 2 cm. During the electrolysis the transition Cd and Cu wire starts to dissolve and give Cd and Cu ions, which were electrochemically reacted with $NaHCO_3$ to give solid CdO/CuO. The obtained solid CdO/CuO was washed with double distilled water till complete removal of unreacted $NaHCO_3$. The solid CdO/CuO was centrifuged and calcinated for 2 hr at 800 °C for dehydration and for the removal of hydroxides to get CdO/CuO nanocomposite. The pH of the dye solution before and after electrolysis was measured and found to be alkaline. The mechanism for the synthesized CdO/CuO nanocomposite is given in Scheme 1.

*Corresponding Author:*bmvenkatesha123@gmail.com*(B.M. Venkatesha)

https://doi.org/10.30799/jnst.337.22080401

Cite this Article as: H.S. Sindhushree, K.M. Chaithra, B.M. Venkatesha, Electrochemical synthesis and characterization of CdO/CuO nanocomposite: Photocatalytic degradation kinetics of indigo carmine dye and its antimicrobial-anticancer activities, J. Nanosci. Tech. 8(4) (2022) 967–971.

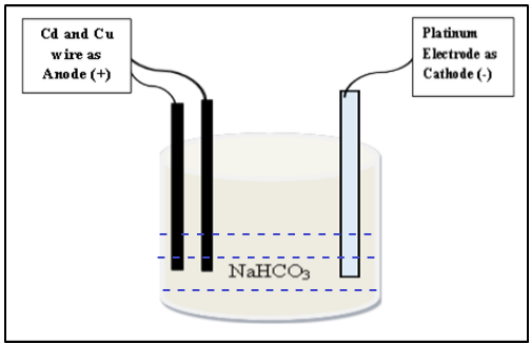

Fig. 1 Experimental set up for the electrochemical synthesis of CdO/CuO nanocomposite

$$Cd \rightleftharpoons Cd^{2+} + 2e^-$$

$$Cu \rightleftharpoons Cu^{2+} + 2e^-$$

$$4\,NaHCO_3 + 4\,e^- \rightleftharpoons 4CO_2 + 4Na^+ + 2OH^-$$

$$Cd^{2+} + 2OH^- \rightleftharpoons Cd(OH)_2$$

$$Cu^{2+} + 2OH^- \rightleftharpoons Cu(OH)_2$$

Overall reaction,

$$Cd + Cu + 4NaHCO_3 \rightleftharpoons Cd(OH)_2 + Cu(OH)_2 + 4CO_2 + 4Na^+$$

$$Cd(OH)_2 + Cu(OH)_2 \xrightarrow{\text{Heat } 800^\circ C} CdO/CuO\ \text{Nanocomposite}$$

Scheme 1 Mechanism for the electrochemical synthesis of CdO/CuO Nanocomposite

3. Results and Discussion

3.1 UV-Visible Spectra

It is clear from the optical absorption spectra, the synthesized CdO/CuO nanocomposite has showed that maximum intensity peak at 249.78 nm in the UV-region and there is no absorption peak in the visible region (Fig. 2). The UV-visible spectrum of CdO/CuO nanocomposite over the range 200-700 nm showed that the synthesized nanocomposite are photoactive under ultraviolet radiation. The band gap of CdO/CuO nanocomposite was calculated using Tauc plot [15] by plotting $(\alpha h\nu)^{1/2}$ verses $h\nu$ (Fig. 2B). The band gap energy could be thus estimated as 4.56 eV for CdO/CuO nanocomposite.

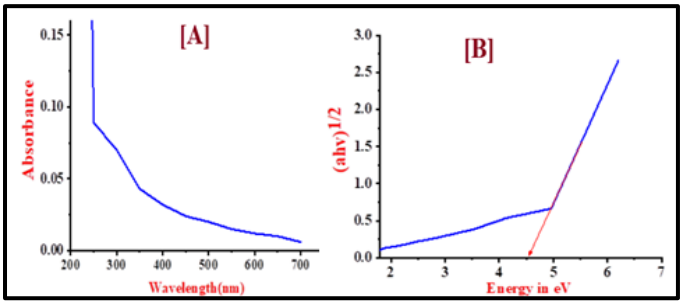

Fig. 2 UV-Visible spectra (A) and Tauc plot (B) of CdO/CuO nanocomposite

3.2 X-Ray Diffraction

The purity and crystallinity of the synthesized CdO/CuO nanocomposite were examined by using powder X-ray diffraction (XRD) as shown in Fig. 3. The peak positions appearing at 2 theta are 33.00, 35.52, 38.33, 55.30, 65.94, 69.27 which can be readily indexed as (001), (010), (110), (111), (200) and (020) crystal planes of the bulk CdO/CuO nanocomposite The reflections are in good conformity with standard JCPDS data for CdO (Card No: 05-0640) and for CuO (Card No: 05-0661). All these diffraction peaks can be perfectly indexed to cubic crystal structure. The crystal size was found to be 49.56 nm from the XRD pattern using the Debye-Scherrer's formula [16], $D=k\lambda/\beta\cos\theta$, where k is an empirical constant equal to 0.9, λ is the wavelength of the X-ray source, β is the full width at half maximum of the diffraction peak and θ is the angular position of the peak. Thus XRD analysis clearly indicates the presence of CdO/CuO as nanocomposite.

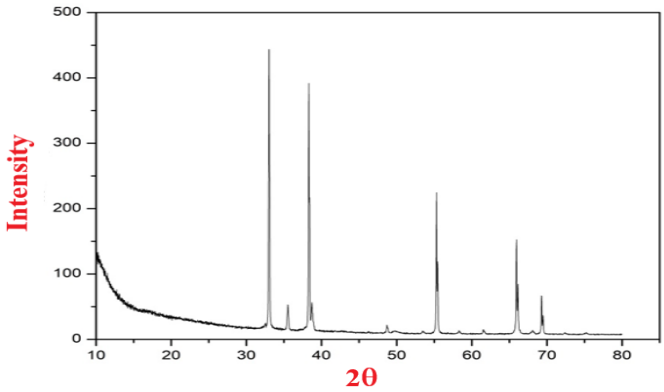

Fig. 3 XRD pattern of CdO/CuO nanocomposite

3.3 Scanning Electron Microscopy

The surface morphology of the synthesized samples was observed by using SEM micrographs. The SEM image of CdO/CuO nanocomposite consists of agglomerated particles (Fig. 4). Energy-dispersive X-Ray spectroscopy (EDS) images are given in Fig. 5. The elements which are present and their relative proportions or quantitative results can be obtained by SEM-EDS analysis (Table 1).

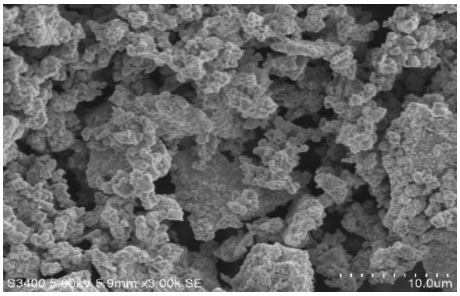

Fig. 4 SEM images of electrochemically synthesized CdO/CuO nanocomposite

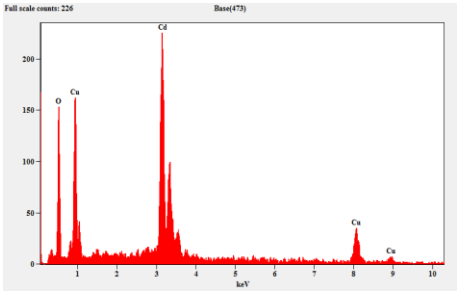

Fig. 5 Energy dispersive X-ray analysis spectrum of electrochemically synthesized CdO/CuO nanocomposite

Table 1 Quantitative results for synthesized CdO/CuOnanocomposite

Element Line	Weight%	Weight% SD	Atom%
O K	33.64	± 1.68	74.06
Cu K	21.35	± 2.59	11.84
Cd L	45.00	± 1.91	14.10

3.4 Photo Degradation Kinetics and COD Measurements

3.4.1 Effect of Concentration of Indigocarmine

The photo degradation process was performed with different concentrations of indigo carmine dye solution ($1x10^{-5}$ to $4x10^{-5}$ M) with constant weight of CdO/CuO nanocomposite is acting as a catalyst. The change in concentration of the indigo carmine was reported by change in colour using spectrophotometer. A plot of log T (percentage transmittance of light) versus time was linear up to 60% of the reaction indicating the disappearance of indigo carmine follows first order kinetics (Fig. 6). The reaction rate decreased with increase in the concentration of indigo carmine. The reason beyond that is with increase in the dye concentration, the solution becomes more intense coloured and the path length of the photons entering the solution is decreased and the few photons reached the catalyst surface. Hence the production of hydroxyl radicals is reduced. Therefore, the photodegradation efficiency is reduced. The pH before and after degradation has been reported. It is observed that after degradation the pH of the dye solution is slightly decreased. To account for the mineralization of dye solution, COD was examined at different stage. The

https://doi.org/10.30799/jnst.337.22080401

Cite this Article as: H.S. Sindhushree, K.M. Chaithra, B.M. Venkatesha, Electrochemical synthesis and characterization of CdO/CuO nanocomposite: Photocatalytic degradation kinetics of indigo carmine dye and its antimicrobial-anticancer activities, J. Nanosci. Tech. 8(4) (2022) 967–971.

formation of different radical species during photo degradation is given in Scheme 2. The indigo carmine dye was found to have mineralized into H_2O, CO_2 and simpler inorganic salts [17, 18], after being irradiated for 5 hrs using CdO/CuO photocatalysts. The photo degradation efficiency of the photocatalyst was calculated by the following formula,

$$\text{Photodegradation efficiency} = \frac{\text{Initial COD} - \text{Final COD} \times 100}{\text{Initial COD}}$$

$$e^-_{cb} + O_2 \longrightarrow O^-_2$$

$$h^+_{vb} + H_2O \longrightarrow H^+ + \cdot OH$$

$$O^-_2 + H^+ \longrightarrow HO^-_2$$

$$HO^-_2 + e^-_{cb} + H^+ \longrightarrow H_2O_2$$

$$H_2O_2 + O^-_2 \longrightarrow \cdot OH + {}^-OH + O_2$$

$$\cdot OH + \text{Dye} \longrightarrow CO_2 + H_2O + \text{Simple inorganic salts}$$

Scheme 2 Photodegradation mechanism of indigocarmine dye using CdO/CuO nanocomposite

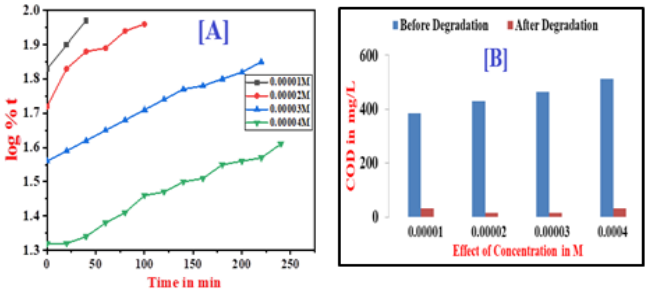

Fig. 6 Effect of concentration of indigocarmine dye on rate of degradation [A] and COD Value [B]

3.4.2 Effect of Catalyst Loading

The experiments were performed by taking different amount of catalyst varying from 0.01 to 0.04 g keeping dye concentration constant in order to study the effect of catalyst loading. The study showed that increase in catalyst loading from 0.01 to 0.04 g increased dye removal efficiency. Further increase in catalyst above 0.04 g decreased the photoactivity of the catalyst, due to aggregation of CdO/CuO nanocomposite at higher concentration causing a decrease in the number of active sites on catalyst surface and increase in the light scattering of CdO/CuO nanocomposite at high concentration [19, 20]. This tends to decrease the passage of light through the sample. Further, the present study indicated, from economic point of view, the optimized photocatalyst loading is 0.02 g/20 mL (Fig. 7). The COD effect has been reported in Fig. 7.

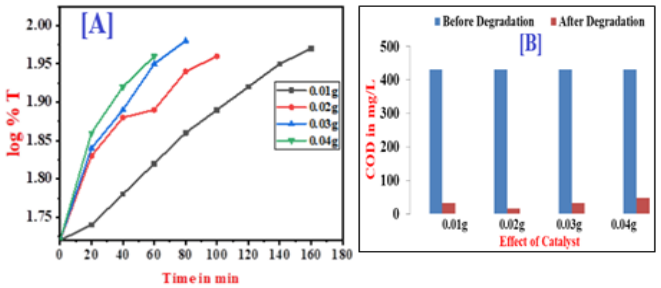

Fig. 7 [A] Effect of catalyst loading on the rate of degradation and [B] COD values of dye solution under UV light

3.4.3 Effect of pH

The pH of the solution is one of the important factors in evaluating the photo degradation reaction in aqueous medium. In the present study, the pH of the solution was adjusted by adding 0.01 M HCl solution and 0.01 M NaOH. The effect of pH was studied at pH 4.0, pH 6.7, pH 8.0 and pH 10.0 by keeping all other experimental conditions constant. The results are reported in Fig. 8. From the results it is observed that the rate of photodegradation increases from pH 4.0 to pH 10.0, the rate of degradation increases with increasing pH. Also, the amount of catalyst recovered after the experiment was lowered at lower pH because of the dissolution of the semiconductor oxides at very low pH values. COD effect are reported in Fig. 8. The optimum pH selected is 6.7 at which photodegradation is high.

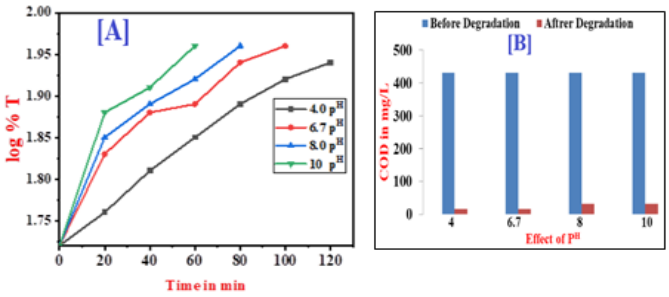

Fig. 8 [A] Effect of pH on the rate of degradation and [B] COD values of dye solution under UV light

3.4.4 Effect of Temperature

Temperature is one of the essential factors which effect the rate of photodegradation. It is clear that the increase in temperature increases the degradation efficiency. However, the reaction is more significantly influenced at high temperature since the diffusion rate increased with temperature, an increase of temperature could bring about an increase in the degradation rate. The rate constant and COD values are reported in Fig. 9 and thermodynamic parameters were calculated and are reported in Table 2.

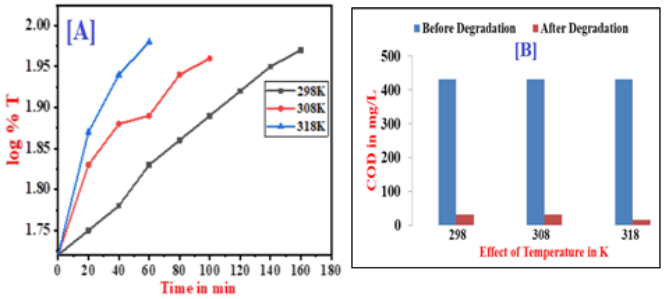

Fig. 9 [A] Effect of temperature on the rate of degradation and [B] COD values of dye solution under UV light

Table 2 Thermodynamic parameters for Indigocarmine dye

Temperature K	ΔH# kJ/mol	ΔS# J/K/mol	ΔG# kJ/mol	Ea
298	36.38	-203.46	97.01	38.68 kJ
308	36.30	-205.35	99.54	(9.289×10^3
318	36.22	-203.97	101.08	Calories)

3.5 Effect of Light Intensity

The photo degradation rate constant in UV light is compared with sunlight. It is perceived that the photo degradation rate constant is increased in UV light compared to sunlight for prepared CdO/CuO nanocomposite. The reason beyond that is when a photon occurrence on a semiconductor (CdO/CuO) energy that overtake the band gap energy of the semiconductor. An electron jumps from the valence band to the conduction band leaving a hole in the valence band .The excited state conduction band electrons and valence band hole can recombined and dissipate energy in the form of heat and get trapped into the metastable surface states, respectively with electrons acceptors and donors that happened to be adsorbed on the semiconductor surface. The stored energy is dissipated within a few nanoseconds by recombination in the absence of suitable e^-/h^+ scavengers. If a suitable scavenger is available to trap the electron recombination is prevented i.e. subsequent redox reaction may occur. Therefore, the nickel oxide nanoparticles act as a very good photocatalyst and is active under UV light compared to sunlight. The rate constant for degradation in sunlight and COD effect are given in Table 3.

Table 3 Effect of rate of degradation in sunlight

Catalyst 0.02 g	Concentration of indigo carmine in M	10^4 k Sec^{-1}	COD Values in mg/L		Photodegradation Efficiency %
			Before degradation	After degradation	
CdO/CuO nanocomposite	2×10^{-5}	0.259	432	32	92.59

3.6 Reuse of Catalyst

The reuse of photocatalyst was examined to see the photodegradation efficiency of the indigo carmine dye solution. After the degradation of dye, the dye sample was kept outside without exposure to the UV-light for 9 hrs and supernatant liquid sample was decanted. The catalyst was thoroughly washed with double distilled water and reused for the photodegradation

https://doi.org/10.30799/jnst.337.22080401

Cite this Article as: H.S. Sindhushree, K.M. Chaithra, B.M. Venkatesha, Electrochemical synthesis and characterization of CdO/CuO nanocomposite: Photocatalytic degradation kinetics of indigo carmine dye and its antimicrobial-anticancer activities, J. Nanosci. Tech. 8(4) (2022) 967–971.

by taking new indigo carmine dye solution. The reuse of photocatalyst shown almost same degradation efficiency compared to the fresh sample. This recommends that the photocatalyst can be regenerated and reused.

3.7 Antimicrobial Activity

Test bacterial cultures were procured from Microbial Type Culture Collection (MTCC) of Institute of Microbial Technology, Chandigarh. Cultures of Gram positive bacteria Staphylococcus aureus (MTCC 7443), *Bacillus subtilis* (MTCC 121) and Gram-negative *Salmonella typhi* (MTCC 7410) and *Pseudomonas aeruginosa* (MTCC 1036) were grown on nutrient agar media used for antibacterial activity assay [21,22]. Chloramphenicol was considered as standard (Table 4).

Table 4 Zone of inhibition in mm against different pathogens for antimicrobial activity

S.No.	Isolate No	*S. aureus*	*B. subtilis*	*S. typhi*	*P. aeruginosa*
1	CdO/CuO	8 mm	9 mm	8 mm	9 mm
2	Chloramphenicol	14 mm	15 mm	14 mm	14 mm

Test microbial inoculums for MIC antibacterial assay were prepared according to Clinical Laboratory Standards Institute (CLSI, 2005). For the growth method, a loop is used to touch the top of three to five colonies of the same morphological type from an agar plate culture. This is suspended in 10 mL of a sterile Mueller Hinton broth (MHB) aseptically and incubated at 37 °C. The turbidity of the actively growing cells were adjusted to the 0.5 McFarland standard (at 625 nm, 0.08-0.01 absorbance in UV-VIS Spectrophotometer) using sterile broth to produce a standardized microbial of approximately 1-2×10^8 CFU/mL. 25-100 mg/mL of 100 µL is added to each plate for studying minimum inhibitory concentration at 625 nm. Fig.10 shows the growth inhibition (Table 5). Compound inhibited the bacterial growth by the clear inhibition zone.

Table 5 Minimum inhibitory concentration (MIC) of different pathogens for antimicrobial activity

Compound	*S. aureus*	*B. subtilis*	*S. typhi*	*P. aeruginosa*
25 mg/mL	27.47	43.95	67.03	86.81
50 mg/mL	19.75	49.38	70.37	87.65
75 mg/mL	9.52	33.33	51.19	78.02
100 mg/mL	11.25	22.5	60.0	80.0

Fig. 10 Zone of inhibition against a) *S. aureus*, b) *B. subtilis* and c) *S. typi* and d) *P. aeruginosa* bacteria

3.8 Anticancer Assay (MTT Assay)

The MCF-7 were seeded in 96 wells plate containing 100 µL of DMEM (high glucose) media, and allowed to grow. After 2 days, 100, 50 and 25 mg/mL of sample were dissolved in 100 µL of 100% DMSO. Then these cells were treated with varying doses of samples and observed after 24 hours. 10 µL of MTT reagent was added to the 96 wells plate and left for 3 to 4 hours. After that media was removed from 96 wells plate and 50 µL of 100% DMSO was added to each well and shaken for 10 seconds. Then absorbance was measured at 570 nm using a multi-well plate reader.

The anticancer activity of CdO/CuO nanocomposite were exposure to MCF-7 cell line at the concentration of 25 mg, 50 mg, 75 mg and 100 mg per mL for 72 hours (Table 6). The anticancer activity reduced the cell viability at different concentration. 100 mg/mL shows the significant result of 88.33% of inhibition against MCF-7 cell lines as concentration decreases the viability increases upto 25 mg/mL. The CdO/CuO shows the IC-50 value of 386.8 which is significantly showing anticancer activity on MCF-7 cell line.

Table 6 Percentage of inhibition and IC-50 values of MCF-7 cell lines and anticancer activity through MTT assay

Concentration of CdO/CuO in mg/mL	% of inhibition of MCF-7 cell	IC- 50 Value
25	38.33	
50	56.66	386.83
75	65.0	
100	88.33	

4. Conclusion

In the present work, the CdO/CuO nanocomposites were synthesized by electrochemical method. The photodegradation by this semiconductor offers a green technology for removal of organic dyes present in waste water and industrial effluents. The photocatalytic study for the synthesized CdO/CuO nanocomposite were investigated by the kinetics of photodegradation of indigo carmine dye by using UV light. Kinetics of photodegradation of indigo carmine dye recommended that the dematerialization of dye follows first order kinetics. The photodegradation rate is low in sunlight when compare to UV light, hence the synthesized CdO/CuO nanocomposites act as a very good photocatalyst and is active under UV light. The complete degradation of dye solution was confirmed by COD measurement. The COD values revealed that 95-96% of the dye had been degraded. The synthesized nanoparticles show appreciably good inactivation of different strains of bacteria.

Acknowledgements

The authors are grateful to late Prof. S. Ananda, Former Professor and chairman, UGC-BSR faculty fellow, DOS in Chemistry, Manasagangothri, University of Mysore, Mysuru, for keen encouragement and timely guidance. Authors also are acknowledges Yuvaraja's college, IOE, UPE & CPEPA, University of Mysore, Karnataka, India.

References

[1] Subhash Kondawar, Ritu Mahore, Ajay Dahegaonkar, Shikha Agrawal, Electrical conductivity of cadmium oxide nanoparticles embedded polyaniline nanocomposites, Adv. Appl. Sci. Res. 2(4) (2011) 401-406.
[2] S. Muruganandam, G. Anbalagan, G. Murugadoss, Optical, electrochemical and thermal properties of co–doped CdS nanoparticles using polyvinylpyrrolidone, Appl. Nanosci. 5 (2015) 245–253.
[3] Karim H. Hassan, Arrej A. Jarullah, Sally K. Saadi, Synthesis of copper oxide nanoparticle as an adsorbent for removal of Cd (II) and Ni (II) Ions from binary system, Int. J. Appl. Env. Sci. 12 (2017) 1841-1861.
[4] S.M. Nomanbhay, K. Palanisamy, Removal of heavy metal from industrial wastewater using chitosan coated oil palm shell charcoal, Elect. J. Biotech. 8 (2005) 43-53.
[5] K. Tam, Antibacterial activity of ZnO nanoroads prepared by hydrothermal method, Thin solid Films 516 (2008) 6167-6174.
[6] I. Ghodbane, L. Nouri, O. Hamdaoui, M. Chiha, Kinetic and equilibrium study for the sorption of cadmium (II) ions from aqueous phase by eucalyptus bark, J. Hazard. Mater. 152 (2008) 148-158.
[7] K. Nithya, P. Yuvasree, N. Neelakandeswari, N. Rajasekaran, K. Uthayarani, et al., Preparation and characterization of copper oxide nanoparticles, Int. J. ChemTech Res. 6 (2004) 2220-2222.
[8] Zafer Serbetçi, Synthesis and optical properties of uranium- doped cadmium oxide synthesized by sol-gel method, Mater. Sci. Pol. 38 (2020) 23-27.
[9] Y.K. Liu, J.A. Zapien, C.Y. Geng, Y.Y. Shan, C.S. Lee, et al., High-quality CdS nanoribbons with lasing cavity, Appl. Phys. Lett. 85 (2004) 3241–3243.
[10] R. Henríquez, P. Grez, E. Muñoz, E.A. Dalchiele, R.E. Marotti, H. Gómez, Template-free non-aqueous electrochemical growth of CdO nanorods, Thin Solid Films 520 (2011) 41–46.
[11] S. Kumar, A.K. Ojha, B. Walkenfort, Cadmium oxide nanoparticles grown in situ on reduced graphene oxide for enhanced photocatalytic degradation of methylene blue dye under ultraviolet irradiation, J. Photochem. Photobiol. B Biol. 159 (2016) 111– 119.
[12] L.E. Brus, Electronic wave functions in semiconductor clusters: experiment and theory, J. Phys. Chem. 90 (1986) 2555–2560.

https://doi.org/10.30799/jnst.337.22080401

Cite this Article as: H.S. Sindhushree, K.M. Chaithra, B.M. Venkatesha, Electrochemical synthesis and characterization of CdO/CuO nanocomposite: Photocatalytic degradation kinetics of indigo carmine dye and its antimicrobial-anticancer activities, J. Nanosci. Tech. 8(4) (2022) 967–971.

[13] M. Lei, K. Bi, Y.B. Zhang, Highly selective growth of TiO_2 nanoparticles on one tip of CdS nanowires, J. Alloys Comp. 646 (2005) 1004–1008.
[14] C.Z. Yao, B.H. Wei, L.X. Men, H. Li, Q.J. Gong, et al., Controllable electrochemical synthesis and photovoltaic performance of ZnO/CdS core–shell nanorod arrays on fluorine-doped tin oxide, J. Power Sour. 207 (2012) 222–228.
[15] S. Gupta, D. Patidar, N.S. Sexena, K.B. Sharma, T.P. Sharma, Electrical study of Cu-CdS and Zn-CdS schottky junction, Adv. Mater. 2(4) (2008) 205-208.
[16] K.R. Raksha, Sannaiah Ananda, An investigation on kinetics of photocatalysis, electrical property and biological activity of electrochemically synthesized ZnS and Ru: ZnS nanophotocatalysts, J. Applicable Chem. 3 (2014) 397-412.
[17] L. Wei, C. Shifu, Z. Wei, Z. Sujuan, Titanium dioxide mediated photocatalytic degradation of methamidophos in aqueous phase, J. Hazard. Mater. 164 (2009) 154-160.
[18] Rakesh, Sannaiah Ananda, Netkal M. Made Gowda, Kithanakere Ramesh Raksha Synthesis of niobium doped ZnO nanoparticles by electrochemical method: Characterization, photodegradation of indigo carmine dye and antibacterial study, Adv. Nanopart. 3 (2014) 133-147.
[19] B. Kraeutler, A.J. Bard, Heterogeneous photocatalytic decomposition of saturated carboxylic acids on TiO_2 powder, Decarboxylative route to alkanes, J. Am. Chem. Soc. 100 (1978) 5985–5992.
[20] H.C. Charan Kumar, R. Shilpa, V. Ravi Shankar Rai, Sannaiah Ananda, Synthesis and characterization of NiO nanoparticles by electrochemical method: photodegradation kinetics of indigo carmine dye and study of antibacterial activities of NiO nanoparticles, J. Appl. Chem. 8 (2019) 622-633.
[21] Khawlah Salah Khashan, Ghassan Mohammad Sulaiman , Farah Abdul Kareem Abdul Ameer, Giuliana Napolitano, Synthesis, characterization and antibacterial activity of colloidal NiO nanoparticles, J. Pharm. Sci. 29 (2016) 541-546.
[22] T.P. Sharma, D. Patidar, N.S. Saxena, K. Sharma, Measurement of structural and optical band gaps of $Cd^{1-x}Zn_xS$ (x = 4 and 6) nanomaterials, Ind. J. Pure Appl. Phys. 44 (2006) 520-615.

https://doi.org/10.30799/jnst.337.22080401

Cite this Article as: H.S. Sindhushree, K.M. Chaithra, B.M. Venkatesha, Electrochemical synthesis and characterization of CdO/CuO nanocomposite: Photocatalytic degradation kinetics of indigo carmine dye and its antimicrobial-anticancer activities, J. Nanosci. Tech. 8(4) (2022) 967–971.